J Mol Model (2013) 19:551–558
DOI 10.1007/s00894-012-1562-5

ORIGINAL PAPER

Coarse-grained simulations for organic molecular liquids based on Gay-Berne and electric multipole potentials

Peijun Xu · Hujun Shen · Lu Yang · Yang Ding · Beibei Li · Ying Shao · Yingchen Mao · Guohui Li

Received: 22 May 2012 / Accepted: 6 August 2012 / Published online: 9 September 2012

Abstract Coarse-grained studies of CH_3SH, CH_3CHO and $CHCl_3$ liquids, based on anisotropic Gay-Berne (GB) and electric multipole potentials (EMP), demonstrate that the coarse-grained model is able to qualitatively reproduce the results obtained from the atomistic model (AMOEBA polarizable force field) and allows for significant saving in computation time. It should be pointed out that the accuracy of the coarse-grained model is very sensitive to how well the anisotropic GB particle is defined and how satisfactorily the EMP sites are chosen.

Keywords *Ab initio* QM · AMOEBA force field · Coarse-grained model · Diffusion coefficient · Radial distribution function

Introduction

With the rapid growth of computation power of computers, molecular mechanic (MM) force fields, such as CHARMM [1, 2], AMBER [3, 4], OPLS [5, 6], GROMOS [7, 8], and so on, have emerged and been used widely to study molecular liquids and biological systems [9–11]. Since nonpolarizable force fields only describe the electrostatic interactions solely in terms of fixed charges [12–14], a variety of polarizable force fields, such as AMOEBA [15, 16], ABEEM/MM [17] and others [18–20], have been proposed including multipole moments and polarization response to the environments.

Even though the above atomistic force fields provide accurate descriptions about the behavior of a system of interest, it is still very expensive or even impossible to surpass the barrier set by the timescale of microsecond and above, as well as the complexity of the biological systems containing millions of atoms. Therefore, a variety of CG models [21–28] have emerged to overcome the obstacle. Nowadays, different coarse-graining strategies [29, 30] have been adopted with a reasonable balance between accuracy and efficiency for different purposes or different applications, enabling one to simulate much longer time scales and larger systems to learn the interesting phenomena that are inaccessible to all-atom models.

In CG models, a group of atoms in a molecule is clustered into a CG site such that the number of degrees of freedom of the molecule is greatly reduced. In most CG models, the coarse-grained particle is assumed to have a spherical shape with fixed point charge, so that the van der Waals (vdW) intermolecular interactions are usually described by Lennard-Jones potential while the Coulomb potential is used to describe the electrostatic interaction. However, because those models treat the coarse-grained particle as a sphere with fixed point charge the calculations of van der Waals (vdW) and electrostatic interactions could be too approximate, limiting the applicability of the traditional CG models to investigate a broad range of molecular systems. In order to improve the accuracy of the coarse-grained calculations of non-bonded interactions, Golubkov and Ren [31] suggested that it should be better to take into consideration the anisotropic shape of the CG particle that can be characterized correctly by an anisotropic potential,

Peijun Xu and Hujun Shen contributed equally to this work

Electronic supplementary material The online version of this article (doi:10.1007/s00894-012-1562-5) contains supplementary material, which is available to authorized users.

P. Xu · H. Shen · L. Yang · Y. Ding · B. Li · G. Li (✉)
Laboratory of Molecular Modeling and Design,
State Key Laboratory of Molecular Reaction Dynamics,
Dalian Institute of Chemical Physics,
Chinese Academy of Sciences,
Dalian 116023 Liaoning Province, People's Republic of China
e-mail: ghli@dicp.ac.cn

P. Xu · L. Yang · Y. Ding · B. Li · Y. Mao (✉)
School of Physics and Electronic Technology,
Liaoning Normal University,
Dalian 116029 Liaoning Province, People's Republic of China
e-mail: myc@lnnu.edu.cn

Y. Shao
Physics of Department, Dalian Maritime University,
Dalian 116026 Liaoning Province, People's Republic of China

then the anisotropic Gay-Berne potential [32, 33] is employed not only to describe the ellipsoid but also to represent the rigid bodies with other shapes, such as sphere and disk. In addition, electric multipole effects of the CG particle should be considered for the multipole expansion (including the charge, dipole moment and quadrupole moment) that gives the charge distribution more accurately than the fixed point charge for the CG particle.

The anisotropic CG model based on the Gay-Berne potential (GB) and electric multipole potential (EMP), termed as GBEMP, has been developed and applied to study a few molecular liquids [31, 34], such as water, methanol and benzene. Recently, GBEMP model has been successfully extended to study polyalanine folding [35].

In our previous work [36], we have employed the on-center GBEMP model (both the GB and EMP sites are placed at the location of the center of mass of the molecule) to study a few organic molecular systems. Even though the on-center GBEMP model can obtain the results of some molecular liquids in good agreement with atomistic study, its performance in simulating some other hydrogen-bonding liquids is unsatisfactory [34]. In order to improve the performance of the GBEMP model in the simulations of hydrogen-bonding liquids, the off-center GBEMP model was proposed [34]. In this study, we are to employ the off-center GBEMP model (the EMP site is placed at the position away from the center of mass) to study three polar molecular (methylsulfide: CH_3SH, acetaldehyde: CH_3CHO and chloroform: $CHCl_3$) liquids.

Model and methods

AMOEBA force field for $CHCl_3$ and its atomistic simulations

From the current AMOEBA force field, one cannot find parameters for $CHCl_3$, so it is necessary to construct AMOEBA force field for $CHCl_3$ in order to perform the atomistic simulation. The initial structure of $CHCl_3$ constructed from GaussView [37] was optimized using GAUSSIAN 03 package [38] at the quantum mechanics (QM) level of HF/6-31G*, and then single point QM calculation was performed on the optimized structure at a higher QM level of MP2/6-311++G(2d,2p). Multipole values (charge, dipole and quadrupole moments) for each atom were calculated with the GDMA method [39], followed by the optimization of multipole parameters for each atom by fitting to QM electrostatic potential. Parameters for stretching bonds and bending angles are obtained from other force fields such as MM3 [40] or OPLS-AA force field [6]. When all above parameters are determined, initial non-bonded vdW parameters were obtained by fitting to the QM calculation (MP2/6-311++G(2d,2p) level) of $CHCl_3$ homodimer intermolecular energy profiles, and were further refined in following atomistic liquid simulation of $CHCl_3$. The AMOEBA force field (only non-bonded parameters) for $CHCl_3$ is presented in Table S1 of Supporting information.

Gay-Berne and electric multipole potentials

Gay-Berne potential

The GB potential between two CG particles i and j has the form

$$U_{\mathrm{GB}}\left(\hat{u}_i,\hat{u}_j,\hat{r}_{ij}\right)=4\varepsilon\left(\hat{u}_i,\hat{u}_j,\hat{r}_{ij}\right)\times\left[\left(\frac{d_w\sigma_0}{r_{ij}-\sigma\left(\widetilde{u_i,u_j,r_{ij}}\right)+d_w\sigma_0}\right)^{12}-\left(\frac{d_w\sigma_0}{r_{ij}-\sigma\left(\widetilde{u_i,u_j,r_{ij}}\right)+d_w\sigma_0}\right)^{6}\right],$$

the range parameter $\sigma\left(\hat{u}_i,\hat{u}_j,\hat{r}_{ij}\right)$ is written as

$$\sigma\left(\hat{u}_i,\hat{u}_j,\hat{r}_{ij}\right)=\sigma_0\left[1-\left\{\frac{\chi\alpha^2\left(\hat{u}_i\cdot\hat{r}_{ij}\right)^2+\chi\alpha^{-2}\left(\hat{u}_j\cdot\hat{r}_{ij}\right)^2-2\chi^2\left(\hat{u}_i\cdot\hat{r}_{ij}\right)\left(\hat{u}_j\cdot\hat{r}_{ij}\right)\left(\hat{u}_i\cdot\hat{u}_j\right)}{1-\chi^2\left(\hat{u}_i\cdot\hat{u}_j\right)^2}\right\}\right]^{-1/2},\tag{2}$$

where

$$\sigma_0=\sqrt{{d_i}^2+{d_j}^2},\tag{3}$$

$$\chi\alpha^2=\frac{{l_i}^2-{d_i}^2}{{l_i}^2+{d_j}^2},\tag{4}$$

$$\chi\alpha^{-2}=\frac{{l_j}^2-{d_j}^2}{{l_j}^2+{d_i}^2},\tag{5}$$

$$\chi^2=\frac{\left(l_i^2-d_i^2\right)\left(l_j^2-d_j^2\right)}{\left(l_j^2+d_i^2\right)\left(l_i^2+d_j^2\right)},\tag{6}$$

where l and d define the length and breadth of each CG particle, therefore a CG particle can be treated as ellipsoid, disk or sphere.

The total well-depth parameter $\varepsilon(\hat{u}_i, \hat{u}_j, \hat{r}_{ij})$ is written as

$$\varepsilon(\hat{u}_i, \hat{u}_j, \hat{r}_{ij}) = \varepsilon_0 \varepsilon_1^{\nu}(\hat{u}_i, \hat{u}_j)\varepsilon_2^{\mu}(\hat{u}_i, \hat{u}_j, \hat{r}_{ij}), \quad (7)$$

where μ and ν are empirical exponents, and are currently set to 2.0 and 1.0, respectively. The terms of ε_1 and ε_2 are calculated in,

$$\varepsilon_1(\hat{u}_i, \hat{u}_j) = \left[1 - \chi^2(\hat{u}_i \cdot \hat{u}_j)^2\right]^{-1/2}, \quad (8)$$

$$\varepsilon_2(\hat{u}_i, \hat{u}_j, \hat{r}_{ij}) = 1 - \left\{\frac{\chi'\alpha'^2(\hat{u}_i \cdot \hat{r}_{ij})^2 + \chi'\alpha'^{-2}(\hat{u}_j \cdot \hat{r}_{ij})^2 - 2\chi'^2(\hat{u}_i \cdot \hat{r}_{ij})(\hat{u}_j \cdot \hat{r}_{ij})(\hat{u}_i \cdot \hat{u}_j)}{1 - \chi'^2(\hat{u}_i \cdot \hat{u}_j)^2}\right\}, \quad (9)$$

and χ', α' are written as

$$\chi' = \frac{1 - (\varepsilon_E/\varepsilon_S)^{1/\mu}}{1 + (\varepsilon_E/\varepsilon_S)^{1/\mu}}, \quad (10)$$

$$\alpha'^2 = \left[1 + (\varepsilon_E/\varepsilon_S)^{1/\mu}\right]^{-1}. \quad (11)$$

Where ε_0 refers to the well-depth of the cross configuration, ε_E and ε_S are the well depth of end-to-end configuration and the well-depth of side-by-side configuration, respectively. It should be pointed out that the Gay-Berne potential will be equivalent to the Lennard-Jones potential when two particles are treated as spheres.

Electric multipole expansion potential

Charge distribution around a multipole site (EMP site) can be described with electric point multipole expansion:

$$M = (q, d_x, d_y, d_z, Q_{xx}, Q_{xy}, ..., Q_{zz}), \quad (12)$$

where q, d, Q refer to charge, dipole and quadrupole moments of the EMP site, respectively. The interaction energy between two EMP sites i and j can be expressed in the polytensor form:

$$U_{\mathrm{EMP}}(r_{ij}) = M_i^t T_{ij} M_j \quad (13)$$

and

$$T_{ij} = \begin{bmatrix} 1 & \frac{\partial}{\partial x_j} & \frac{\partial}{\partial y_j} & \frac{\partial}{\partial z_j} & \cdots \\ \frac{\partial}{\partial x_i} & \frac{\partial^2}{\partial x_i \partial x_j} & \frac{\partial^2}{\partial x_i \partial y_j} & \frac{\partial^2}{\partial x_i \partial z_j} & \cdots \\ \frac{\partial}{\partial y_i} & \frac{\partial^2}{\partial y_i \partial x_j} & \frac{\partial^2}{\partial y_i \partial y_j} & \frac{\partial^2}{\partial y_i \partial z_j} & \cdots \\ \frac{\partial}{\partial z_i} & \frac{\partial^2}{\partial z_i \partial x_j} & \frac{\partial^2}{\partial z_i \partial y_j} & \frac{\partial^2}{\partial z_i \partial z_j} & \cdots \\ \vdots & \vdots & \vdots & \vdots & \ddots \end{bmatrix} \left(\frac{1}{r_{ij}}\right). \quad (14)$$

On account of the CG particles have anisotropic shapes as given by the GB potential, a so-called polarization catastrophe will occur when interaction in very short range. An effective solution to this problem through the use of a damping function to modify the multipole interaction (<5 Å):

$$\lambda = 1 - \exp(-au^3), \quad (15)$$

where $u = r_{ij} \Big/ (\alpha_i \alpha_j)^{1/6}$ is the effective distance with r_{ij} as the actual distance between sites i and j. The factor a is the damping strength, and is set to 0.39 in the present work.

System minimizations and molecular dynamics (MD) simulations

The cubic liquid boxes containing 125 molecules are constructed by VEGAZZ software [40], and the lengths of sides are 22.65 Å, 22.72 Å and 25.56 Å for liquid CH_3SH, CH_3CHO and $CHCl_3$, respectively. Each atomistic system is minimized for several hundred steps, followed by atomistic NPT simulations with the length of 5 ns. In all atomistic MD simulations, the integration step is set to 1 fs, and a cutoff value of 12 Å is used for non-bonded interactions.

All initial structures of the liquids for CG simulations are converted from their corresponding all-atom models. In each system, the coordinates of all atoms are recorded in a library that enables us to recover the coarse-grained representation of the system back to its atomistic representation for analysis. For each system, minimizations have been carried out for several hundred steps, and the following NPT simulations have been performed for at least 200 ns with the integration step of 10 fs, and a cutoff value of 12 Å is used for non-bonded interactions.

Results and discussion

GB and EMP parameters for small molecules

GB parameters

The determination of GB parameters for small molecules has been described previously [31, 34]. To construct the atomistic energy profiles for the vdW interactions of the homo-dimers, different special configurations for CH_3SH, CH_3CHO and $CHCl_3$ homo-dimers, such as cross-shape, side-by-side, T-shape, end-to-end (or face-to-face), are selected, and are given in Table S2 of Supporting information. The AMOEBA polarizable force field was used to calculate the vdW interaction energies for each homo-dimer with different configurations.

In the calculations, the CG particles of both CH_3SH and CH_3CHO molecules were treated as ellipsoids, while the CG particle of $CHCl_3$ molecule was considered to have disk-like shape. By employing a generic algorithm, the GB parameters were obtained by fitting to the atomistic energy profiles of special configurations in gas phase and were further refined in the following liquid simulations, and the final GB parameters are listed in Table 1.

The vdW interaction energy profiles for CH_3SH, CH_3CHO and $CHCl_3$ obtained from AMOEBA all-atom model and the GB coarse-grained model are shown together in Fig. 1. In Fig. 1a, the vdW interaction energy curves of the CH_3SH homo-dimer given by the GB model on the whole reproduce the results from all-atom model, especially for cross and side-by-side configurations. Although the energy curves of the end-to-end and T-shape configurations are observed to have differences between the CG and all-atom models, previous experiences told us that the end-to-end and T-shape configurations of a rod-like molecule should make less contribution to the accuracy of GB parameters compared to the cross and side-by-side configurations. From Fig. 1b, one can see that only the cross-shape energy curves from CG and all-atom models are fitted well. For other configurations, there are some deviations that are acceptable because the energy differences within 1 kcal mol^{-1} are observed near the bottom of potential wells. In Fig. 1c, it is shown that the interaction energy of the $CHCl_3$ homo-dimers given by the GB model is not accurate compared with all-atom model for face-to-face configuration. On account of the $CHCl_3$ molecule was treated with disk, the CG particle is viewed as an integrated molecule, and the internal information about the rigid body molecule is frozen or screened, so that the mass distribution inside the CG particle is assumed to be uniform. However, in the all-atom model of $CHCl_3$ molecule, one can see that the mass distribution is significantly dominated by one side having atoms of chlorine (Cl). In addition, three chlorines of $CHCl_3$ are indistinguishable in the CG model but are distinguishable in the atomistic model. In this situation, special care should be considered in future works. There are several ideas we are going to test, such as the contributions of the end-to-end and T-shape configurations have to be sacrificed to achieve the best fitting of the face-to-face configuration that has the deepest well-depth, or, the $CHCl_3$ molecule can be treated with more than one CG particle, etc.

Table 1 The GB parameters for CH_3SH CH_3CHO and $CHCl_3$ in GBEMP model

	d (Å)	l (Å)	d_w	ε_0 (kcal/mol)	$\varepsilon_E/\varepsilon_S$
CH_3SH	2.385	3.450	1.250	1.306	0.664
CH_3CHO	2.615	4.050	1.152	0.830	0.599
$CHCl_3$	5.209	2.683	0.757	0.500	1.616

EMP parameters

The atomic electric multipole moments can be directly calculated from the *ab initio* QM methods in gas-phase. However, we need to consider the contribution of induced dipoles to improve the accuracy of the EMP parameters that can be obtained by averaging electric multipole moments in solvent. According to previous works, point multipole sites (EMP sites) are placed on the atoms possessing the most electronegativity. Based on the charge parameters of CH_3SH, CH_3CHO and $CHCl_3$, listed in Table S3 of Supporting information, the EMP sites are placed on the carbon atom (C) of CH_3SH, the oxygen atom (O) of CH_3CHO, and the carbon atom (C) of $CHCl_3$ in this work, respectively, and the final EMP parameters are given in Table 2.

Liquid simulation results

Radial distribution function (RDF)

To evaluate the performance of the GBEMP model for three molecular liquids (CH_3SH, CH_3CHO and $CHCl_3$), the macroscopic properties, such as the radial distribution functions (RDF), liquid densities, self-diffusion coefficients and average potential energies, were calculated and compared to atomistic results. In advance of computing the macroscopic properties, each CG trajectory represented by Euler coordinates was converted into the corresponding atomistic trajectory depicted by Cartesian.

From Fig. 2, excellent agreement between the CG and all-atom models is found for the RDFs of liquid CH_3SH in term of C-C and C-S pairs. Two models arrive at the peaks simultaneously round the separation of 4 Å. The C-C and C-S RDFs of the CG model are in good agreement with those of the all-atom model before the peaks and after the

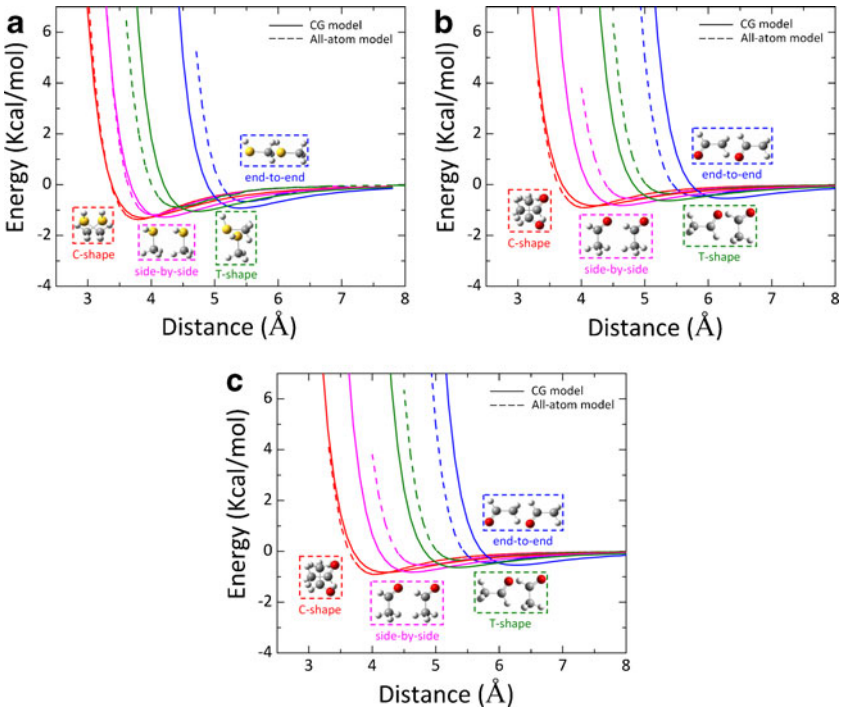

Fig. 1 Comparison of vdW intermolecular interaction energies calculated from the CG and all-atom simulations for (**a**) CH_3SH (**b**) CH_3CHO and (**C**) $CHCl_3$. As for CH_3SH and CH_3CHO (rod-like molecules) the curves of four configurations namely cross shape (*red lines*) end to end (*blue lines*) T-shape (*green lines*) and side by side (*pink lines*) are displayed respectively. As for $CHCl_3$ (disk-like molecule) the curves of three configurations namely face-to-face (*orange lines*) T-shape configurations (*green lines*) side-by-side configuration (*pink lines*) were selected. The results of the CG model are represented with solid lines and the dash lines are the results from the all-atom model

separation of 6 Å, except the atomistic results have demonstrated some fluctuations in the range from 4 to 6 Å. The RDFs in terms of C-H and S-H pairs calculated from the CG simulations are comparable to atomistic results. In the short range from 3 to 6 Å, the deviations between two models in the C-H and S-H RDFs may be ascribed to the multipole effect. From Table S3, one can find that the hydrogen atom of the (SH)- group has negative charge (−0.11359), and increasing the number of multipole sites can improve the result but would sacrifice the efficiency of the CG model. In the long range (after 6 Å), the multipole effects have little impact on the RDFs, so that excellent agreement between CG and all-atom models is observed in both C…H and S…H RDFs.

In Fig. 3, the C-C, C-O and C-H RDFs of the CG model of CH_3CHO have shown good agreement with atomistic results. In the range from 4 to 5 Å, the C-C RDF of the all-atom model exhibits two peaks, and the CG model result displays just clearly one peak, but this is inevitable for the CG model because two carbon atoms are grouped into one site. In Fig. 3, there also is an obvious deviation between two models. The O-H RDF of the all-atom model displays two peaks in the range from 2 to 6 Å, where the peak of the first shell is located at around 2.5 Å and another peak is found at round 5.5 Å. The first shell should be related to the hydrogen atom of the (COH)- group while the second shell is associated with the hydrogen atom of the (CH_3)- group. However, in the CG model, all those hydrogen atoms are united into a CG site, so that the CG model result of the O-H RDF only displays one peak at 4.5 Å.

In the CG simulation of the $CHCl_3$ liquid, only the C-C RDF of the CG model is able to reproduce the all-atom result, shown in Fig. 4. In the short range from 2 to 6 Å, the C-Cl and Cl-Cl RDFs of the CG model have poor

Table 2 The EMP parameters for CH_3SH CH_3CHO and $CHCl_3$ in GBEMP model

	Charge (e)	Dipole moments (Debyes)	Quadrupole moment tensor (Buckinghams)			Inertia (g·Å^2/mol)
C(CH_3SH)	0.0	1.835	−3.216	−3.722	0.203	4.883
		0.950	−3.722	4.552	−0.209	39.220
		−0.041	0.203	−0.209	−1.335	40.935
O(CH_3CHO)	0.0	2.964	3.325	−2.778	0.262	8.857
		−1.560	−2.778	−1.093	0.213	50.427
		0.025	0.262	0.213	−2.231	55.902
C($CHCl_3$)	0.0	0.023	−1.574	0.163	0.054	170.482
		−0.031	0.163	−2.180	0.145	170.482
		−1.358	0.054	0.145	3.754	329.170

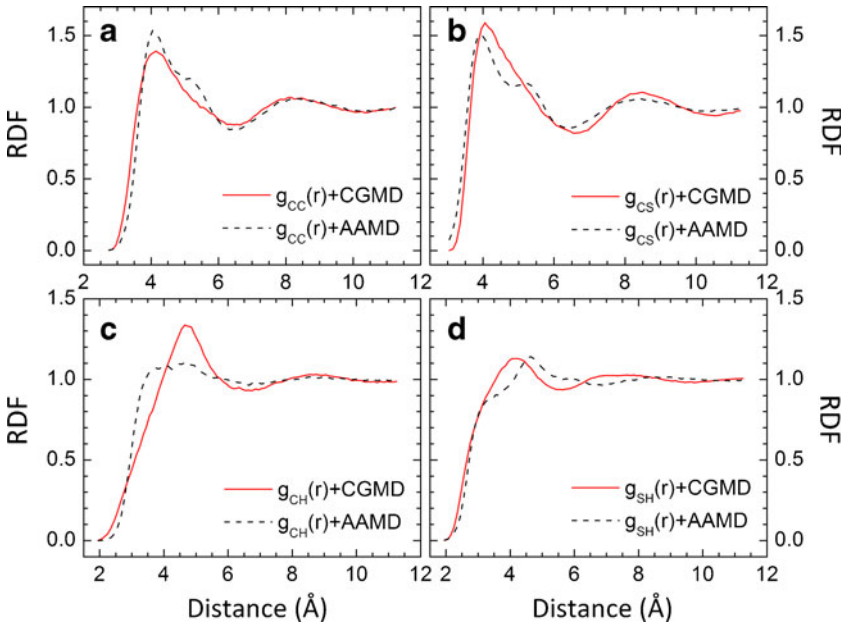

Fig. 2 Comparison of RDFs of C-C C-S C-H and S-H for liquid CH_3SH from up to down obtained from GBEMP coarse-grained (CG) and AMOEBA all-atom (AA) models respectively. The results of the CG model are represented with red solid lines and the black lines correspond to the results of AA model

performance due to the three chlorines being clustered into just one pseudo-atom at the center of mass of $CHCl_3$. Because of the coarse-graining approach, the three chlorines are indistinguishable in the CG model but are distinguishable in the all-atom model. Therefore, the differences between two models for the C-Cl and Cl-Cl RDFs are inevitable if $CHCl_3$ is treated as one GB particle. To improve the performance of the CG model, high resolution coarse-graining approaches are needed, such as treating $CHCl_3$ with two or more GB particles. However, such an approach would impair the efficiency of the CG model.

Finally, the absolute coordination numbers of the first and second salvation shell in RDFs are examined for three organic molecules, and the results are listed in Table S4 of Supporting information. By comparing the coarse-grained results to atomistic calculations, only slight discrepancy was found in the coordination numbers of the first solvation shell for three molecular liquids. As for the second solvation shell, both models give the same results. This indicates that our coarse-grained model is able to quantitatively reproduce the macroscopic property calculated from atomistic model and the differences found in RDFs are unavoidable due to the inherent feature of coarse-graining.

Diffusion constants and average potential energy

In order to investigate other macroscopic properties of CH_3SH, CH_3CHO and $CHCl_3$ liquids, gained through two

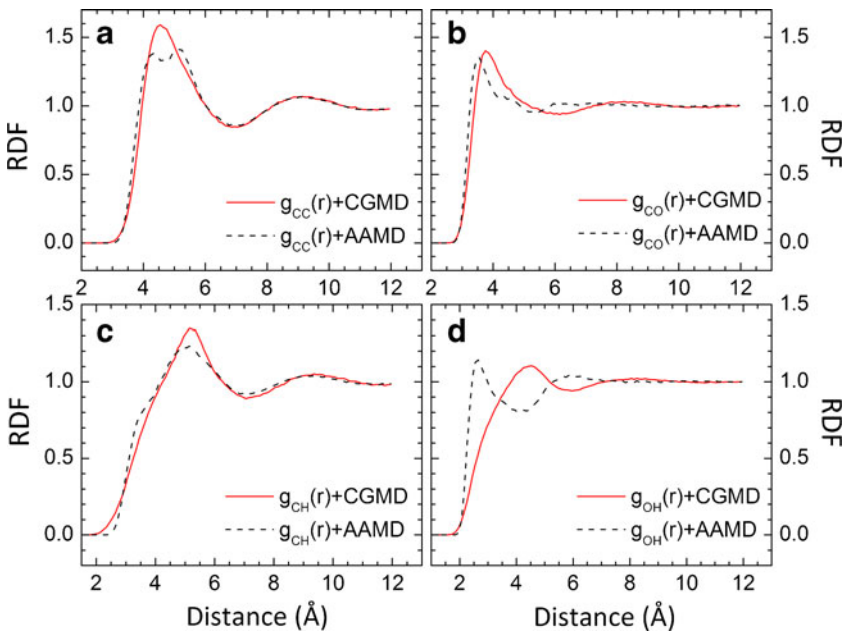

Fig. 3 Comparison of RDFs of C-C C-O C-H and O-H for liquid CH_3CHO from up to down obtained from GBEMP coarse-grained (CG) and AMOEBA all-atom (AA) models respectively. The results of the CG model are represented with red solid lines and the black lines correspond to the results of AA model

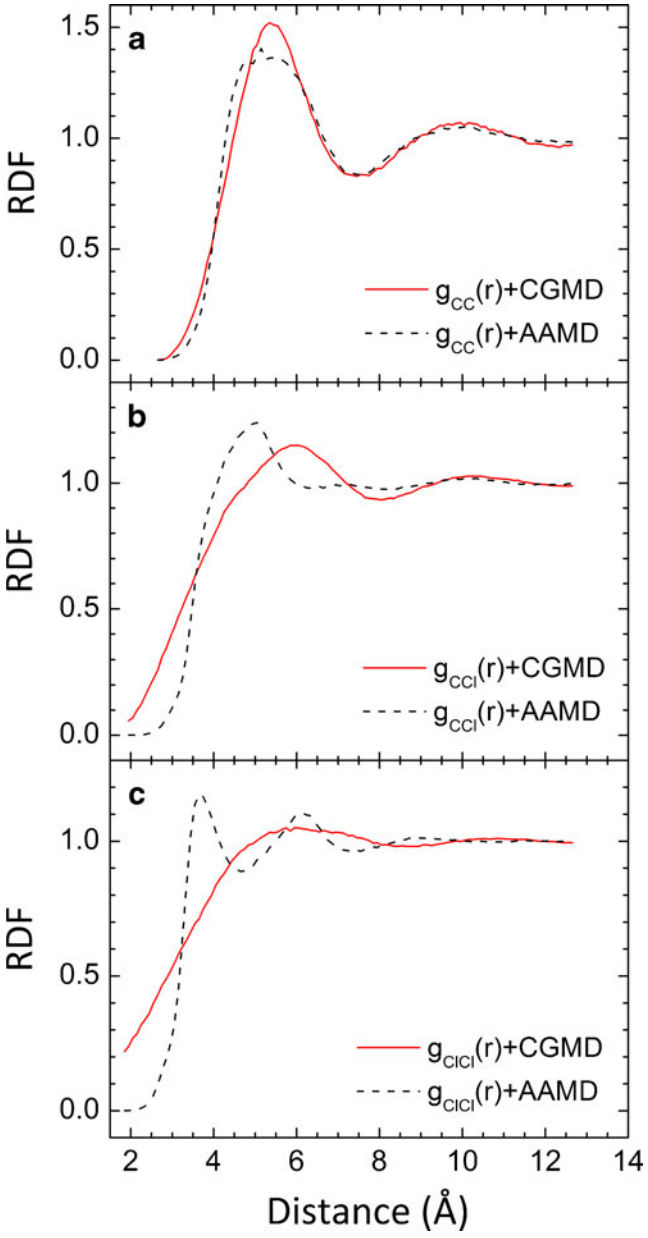

Fig. 4 Comparison of RDFs of C-C C-Cl and Cl-Cl for liquid $CHCl_3$ from up to down obtained from GBEMP coarse-grained (CG) and AMOEBA all-atom (AA) models respectively. The results of the CG model are represented with red solid lines and the black lines correspond to the results of AA model

models, we again have made comparative calculations of self-diffusion coefficients, densities, and average potential energies of three molecular liquids, which are given in Table 3. It presents that the CG model results in general inosculate atomistic or experimental ones, especially for densities. Even though the self-diffusion coefficient for the $CHCl_3$ liquid calculated from the CG simulation is overestimated compared to the experimental value [41], the all-atom (AMOEBA) result exhibits similar behavior. Among three liquids, the $CHCl_3$ liquid displays the largest difference of the self-diffusion coefficient between the CG and all-atom models. As discussed above, the current treatment of the CG model of $CHCl_3$ with one GB particle may be the reason. As for average potential energies, a good agreement between the two models is observed. In order to further examine our coarse-grained model, we have carried out some calculations on the mixtures CH_3CHO:$CHCl_3$ and CH_3SH:CHCl3 (with molar fraction 2:3), respectively, and the results are listed in Table S5 of Supporting information. Similarly, the CG model results are comparable to atomistic results, indicating that our coarse-grained model is able to calculate the solvation free energy with reasonable accuracy.

Conclusions

In this article, a physics-based coarse-grained model, based on anisotropic Gay-Berne and electrostatic multipole potentials, is employed to study the macroscopic properties of three molecular liquids (CH_3SH, CH_3CHO and $CHCl_3$). The CH_3SH and CH_3CHO molecules were treated with ellipsoidal GB particles while the GB particle of $CHCl_3$ was considered to have disk-like shape. In the GBEMP model, GB site is placed at the center of mass of the molecule, and the GB parameters were obtained by fitting to the atomistic calculations of the vdW interaction energies. The EMP sites of the GB particles were placed at the locations of the atoms possessing strong electronegativity, and the EMP parameters were calculated from multipole expansion at the EMP sites including the contribution of induced dipoles in solvent. The RDFs, self-diffusion

Table 3 The self-diffusion coefficients, densities and average potential energies of CH_3SH CH_3CHO and $CHCl_3$ liquids obtained from coarse-grained and atomistic models

	Self-diffusion coefficient (10^{-9} cm^{-2}/s)			Density (g/cm^3)			Potential energy (kcal/mol)	
	Expt.	All-atom.	CG	Expt.	All-atom.	CG	All-atom.	CG
CH_3SH	–	6.3606	6.6144	0.8599	0.8318	0.8607	−3.715	−3.556
CH_3CHO	–	2.0819	2.1135	0.7800	0.7797	0.7842	−6.316	−6.104
$CHCl_3$	2.45±0.04[a]	3.0480	3.4011	1.483	1.447	1.481	−3.844	−3.622

Ref. [41]

coefficients, liquid densities and average potential energies for three molecular liquids were calculated from the MD simulations based on GBEMP CG and AMOEBA all-atom models. In general, the CG results have shown good agreement with atomistic calculations. Although some results from the CG model are unsatisfactory, the development of a coarse-grained model is not to aim at reproducing all atomistic features but to try and reproduce the main atomistic features. In practice, we can increase the accuracy of the coarse-grained model by defining the anisotropic GB particle at higher resolution level or by adding more EMP sites inside the GB particle. Nevertheless, the consequence of such approaches would be to diminish the efficiency of the CG model. In fact, making the effort to find the optimal balance between the accuracy and efficiency is one of the most important goals of developing a coarse-grained model, but it is quite challenging.

Acknowledgments This work is supported by the National High-tech Research and Development Program (2009AA01A137), the National Natural Science Foundation of China (31070641/ C050101), and "Hundred Talents Program of the Chinese Academy Sciences". The work of Y. S. is also supported by the Fundamental Research Funds for the Central Universities of China (2011QN151).

References

1. Nilsson L, Karplus M (1986) J Comput Chem 7:591–616
2. MacKerell AD Jr, Bashford D, Bellott M, Dunbrack RL, Evansek JD, Field MJ, Fischer S, Gao J, Guo H, Ha S, Joseph-McCarthy D, Kuchnir L, Kuczera K, Lau FTK, Mattos C, Michnick S, Ngo T, Nguyen DT, Prodhom B III, Reiher WE, Roux B, Schlenkrich M, Smith JC, Stote R, Straub J, Watanabe M, Wiórkiewicz-Kuczera J, Yin D, Karplus M (1998) J Phys Chem B 102:3586–3616
3. Weiner SJ, Kollman PA, Case DA, Singh UC, Ghio C, Alagona G, Profeta S, Weiner P (1984) J Am Chem Soc 106:765–784
4. Cornell WD, Cieplak P, Bayly CI, Gould IR Jr, Merz KM, Ferguson DM, Spellmeyer DC, Fox T, Caldwell JW, Kollman PA (1995) J Am Chem Soc 117:5179–5197
5. Jorgensen WL, Tirado-Rives J (1988) J Am Chem Soc 110:1657–1671
6. Jorgensen WL, Maxwell DS, Tirado-Rives J (1996) J Am Chem Soc 118:11225–11236
7. Hermans J, Berendsen HJC, van Gunsteren WF, Postma JPM (1984) Biopolymers 23:1513–1518
8. Daura X, Mark AE, van Gunsteren WF (1998) J Comput Chem 19:535–547
9. Onuchic J, Luthey-Schulten Z, Wolynes PG (1997) Annu Rev Phys Chem 48:545–600
10. Dobson CM, Šali A, Karplus M (1998) Angew Chem Int Ed 37:868–893
11. Shakhnovich EI (2006) Chem Rev 106:1559–1588
12. Halgren TA, Damm W (2001) Curr Opin Struct Biol 11:236–242
13. Finney JL (2001) J Mol Liq 90:303–312
14. Rick SW, Stuart SJ (2002) Rev Comput Chem 18:89–146
15. Ren PY, Ponder JW (2003) J Phys Chem B 107:5933–5947
16. Ponder JW, Case DA (2003) Adv Protein Chem 66:27–85
17. Yang ZZ, Wang CS (2003) J Theor Comput Chem 2:273–300
18. Gresh N, Guo H, Salahub DR, Roques BP, Kafafi SA (1999) J Am Chem Soc 121:7885–7894
19. Patel S, Mackerell AD Jr, Brooks CL III (2004) J Comput Chem 25:1504–1514
20. Banks JL, Kaminski GA, Zhou RH, Mainz DT, Berne BJ, Friesner RA (1999) J Chem Phys 110:741–754
21. Akkermans RLC, Briels WJ (2001) J Chem Phys 114:1020–1031
22. Marrink SJ, de Vries AH, Mark AE (2004) J Phys Chem B 108:750–760
23. Zacharopoulos N, Vergadou N, Theodorou DN (2005) J Chem Phys 122:244111
24. Chu JW, Izvekov S, Voth GA (2006) Mol Simul 32:211–218
25. Girard S, Müller-Plathe F (2004) Lect Notes Phys 640:327–356
26. Han W, Wu YD (2007) J Chem Theory Comput 3:2146–2161
27. van den Noort A, den Otter WK, Briels WJ (2007) Europhys Lett 80:28003
28. Hills RD, Brooks CL III (2009) Int J Mol Sci 10:889–905
29. Tozzini V (2005) Curr Opin Struct Biol 15:144–150
30. Voth GA (ed) (2009) Coarse-graining of condensed phase and biomolecular systems. CRC, Boca Raton
31. Golubkov PA, Ren PY (2006) J Chem Phys 125:064103
32. Gay JG, Berne BJ (1981) J Chem Phys 74:3316–3319
33. Cleaver DJ, Care CM, Allen MP, Neal MP (1996) Phys Rev E 54:559–567
34. Golubkov PA, Wu JC, Ren PY (2008) Phys Chem Chem Phys 10:2050–2057
35. Wu JC, Zhen X, Shen HJ, Li GH, Ren PY (2011) J Chem Phys 135:155104
36. Xu PJ, Tang YY, Zhang J, Zhang ZB, Wang K, Shao Y, Shen HJ, Mao YC (2011) Acta Phys Chim Sin 27:1839–1846 (in Chinese)
37. Dennington R, Keith T, Millam J (2009) Semichem Inc, Shawnee Mission KS
38. Frisch MJ, Trucks GW, Schlegel HB, Scuseria GE, Robb MA, Cheeseman JR Jr, Montgomery JA, Vreven T, Kudin KN, Burant JC, Millam JM, Iyengar SS, Tomasi J, Barone V, Mennucci B, Cossi M, Scalmani G, Rega N, Petersson GA, Nakatsuji H, Hada M, Ehara M, Toyota K, Fukuda R, Hasegawa J, Ishida M, Nakajima T, Honda Y, Kitao O, Nakai H, Klene M, Li X, Knox JE, Hratchian HP, Cross JB, Bakken V, Adamo C, Jaramillo J, Gomperts R, Stratmann RE, Yazyev O, Austin AJ, Cammi R, Pomelli C, Ochterski JW, Ayala PY, Morokuma K, Voth GA, Salvador P, Dannenberg JJ, Zakrzewski VG, Dapprich S, Daniels AD, Strain MC, Farkas O, Malick DK, Rabuck AD, Raghavachari K, Foresman JB, Ortiz JV, Cui Q, Baboul AG, Clifford S, Cioslowski J, Stefanov BB, Liu G, Liashenko A, Piskorz P, Komaromi I, Martin RL, Fox DJ, Keith T, Al-Laham MA, Peng CY, Nanayakkara A, Challacombe M, Gill PMW, Johnson B, Chen W, Wong MW, Gonzalez C, Pople JA (2004) Gaussian 03. Gaussian Inc, Wallingford
39. Stone AJ (2005) J Chem Theory Comput 1:1128–1132
40. Pedretti A, Villa L, Vistoli G (2003) Theory Chem Acc 109:229–232
41. Wu C, Siddiq M, Bo SQ, Chen TL (1996) Macromolecules 29:3157–3160